

# Performance of W/Cu FGM based plasma facing components under high heat load test

Zhang-Jian Zhou <sup>\*</sup>, Shu-Xiang Song, Juan Du, Zhi-Hong Zhong, Chang-Chun Ge

*Research Center on Fusion Materials, Laboratory of Special Ceramic and P/M, University of Science and Technology, Beijing 100083, PR China*

---

## Abstract

Three different methods, plasma spraying, infiltration-welding method and resistance sintering under ultra-high pressure, have been developed to fabricate W/Cu FGM based plasma facing components. SEM analysis showed that good grading composition of all FGM samples had been obtained. Water quenching and electron, or laser beam test facilities have been utilized to investigate and compare thermal shock behavior and performance under high heat load. It is found that the grading at the interface between W and Cu is very effective for the reduction of thermal stress. W/Cu FGM fabricated by infiltration-welding method has the best thermal shock resistance among these three kinds of W/Cu FGM. © 2007 Elsevier B.V. All rights reserved.

*PACS:* 61.82.Bg; 68.60.Dv; 28.52.Fa

*Keywords:* Graded materials; Tungsten; Thermal shock; Plasma facing component

---

## 1. Introduction

Cu/W Joints are of interest for potential use in divertor assemblies in fusion reactors [1–4]. For the highest sputtering threshold of all possible candidates, tungsten will be the most likely plasma facing armor materials in highly loaded plasma-interactive components of the next step fusion reactors. Copper based alloys have been proposed as heat sink materials behind the armor due to their high thermal conductivity. During normal operation regimes, the plasma facing components of next step fusion devices will be subjected to intense,

quasi-stationary heat pulses. This will put strong demands on the durable and reliable joining of bulk tungsten to copper to achieve an acceptable component lifetime in a fusion environment. The main problem in the development of W/Cu joints is the large difference in the coefficient of thermal expansion (CTE) and other physical properties between these two materials, which may cause large thermal stress during fabrication and service, and leads to cracking, delaminating and a reduced lifetime of the components by rapid detachment.

The use of interlayer has been shown to be an effective method to join dissimilar materials. Interlayer materials are typically ductile in order to accommodate the otherwise high thermal residual stresses, and it is usually preferable that the thermal

---

<sup>\*</sup> Corresponding author. Fax: +86 10 62332472.  
E-mail address: [zhouzhj@mater.ustb.edu.cn](mailto:zhouzhj@mater.ustb.edu.cn) (Z.-J. Zhou).

expansion behavior of an interlayer material is intermediate between the materials being joined. If the interlayer will be compositionally graded, the stress state and stress singularities would be expected to be different from those for a homogeneous interlayer, thus W/Cu functionally graded materials (FGM) will be a promising solution way for joining W and Cu [5–7]. Due to the large difference in melting point of W and Cu, and the sintering temperature of W much higher than the melting point of Cu, it is not easy to fabricate W/Cu FGM by conventional methods [7–9]. The main problem in the development of W/Cu FGM is the selection of suitable fabrication technologies.

The aim of the present study is the demonstration of the feasibility of producing W/Cu FGM by three investigated metallurgical processes, plasma spraying, infiltration-welding method and resistance sintering under ultra high pressure and the comparison of these methods by analyses of the microstructure and the performance under high heat load. The limitations and advantages of each method are outlined.

## 2. Experiments

### 2.1. Plasma spraying for W/Cu FGM

W Powder with particle size of 45–20  $\mu\text{m}$  and Cu powders with particle size of 76–45  $\mu\text{m}$  were used for plasma spraying. The interlayer coating materials of W/Cu were obtained by mixing W powder and Cu powder with volume ratio of 50:50%. W/Cu Mixtures and W powders were sprayed layer by layer on an oxygen free copper substrate ( $\Phi 70 \text{ mm} \times 5 \text{ mm}$ ) by atmosphere plasma spraying (APS) using a PT-A-3000 S plasma-spray facility made in Sweden. Argon was used as the plasma gas. Argon and nitrogen were used for cooling the substrates and preventing the coatings from oxidation. The thickness of the W/Cu graded layer was 300  $\mu\text{m}$ , and the thickness of pure W coating was 500  $\mu\text{m}$ .

### 2.2. Infiltration-welding process for W/Cu FGM

This process includes three steps: (1) Fabrication of a porous graded W skeleton (with three layers). W powders with different particles size (average particle size of 3, 7, 15  $\mu\text{m}$  and purity of >99.5% for each layer) were mixed separately with different volume of pore-making agent (stearic acid) in an agate mill. The mixed powder were stacked layer

by layer in a steel mould to form a green compact of 30 mm  $\times$  30 mm  $\times$  3 mm, then the compact was put in a graphite crucible embedded with  $\text{Al}_2\text{O}_3$  powder and sintered at 1300  $^\circ\text{C}$  for 1 h under  $\text{H}_2$  atmosphere to form a porous graded W skeleton. (2) Infiltration with liquid Cu in vacuum. The porous sintered W skeleton with a green compact of Cu (cold pressed by Cu powder with particle size of less than 76  $\mu\text{m}$  and purity of >99%) on its top was embedded in  $\text{Al}_2\text{O}_3$  powder. The thickness of the Cu compact was determined according to the requirement of full filling of the pores in the W skeleton and the designed thickness of the full-Cu top layer. Infiltration of the porous graded W skeleton with liquid Cu was realized after heating to 1300  $^\circ\text{C}$  and holding for 30 min. (3) Welding W plate on the W-rich surface of the W/Cu graded layer. The infiltrated specimen was welded with a W93–Ni5–Fe2 heavy alloy plate of 2.5 mm thickness by hot pressing at 900–1000  $^\circ\text{C}$  for 1.5 h under pressure of 20 MPa in Ar atmosphere.

### 2.3. Resistance sintering under ultra high pressure for W/Cu FGM

A novel one step method, named ‘resistance sintering under ultra-high pressure (RSUHP)’, has been developed to fabricate W/Cu FGM without the addition of any sintering additive in author’s laboratory. W powder with particle size of 1  $\mu\text{m}$ , and a purity of more than 99.5%, and Cu powder with particle size less than 45  $\mu\text{m}$ , and a purity of more than 99.9% were used as the starting materials. W and Cu were mixed and milled with different compositions and then were stacked layer by layer in a steel mould to form a green compact of  $\Phi 20 \text{ mm} \times 6 \text{ mm}$ . The W/Cu FGM green compact was placed in the pressure vessel, the detail of the setup can be found in Ref. [10]. First, the pressure was mechanically cubic isostatic loaded on the W/Cu FGM green compact, then an alternating current (A.C.) was applied to the sample, thus heating and sintering of the FGM by Joule heating. The sintering parameters were: under pressures of 8 GPa, an electric power input of about 20 kW and sintering times of 65 s.

## 3. Results and discussion

### 3.1. W/Cu FGM by APS

Fig. 1 shows the SEM backscattered electron image (BEI) of the cross section of W/Cu coating

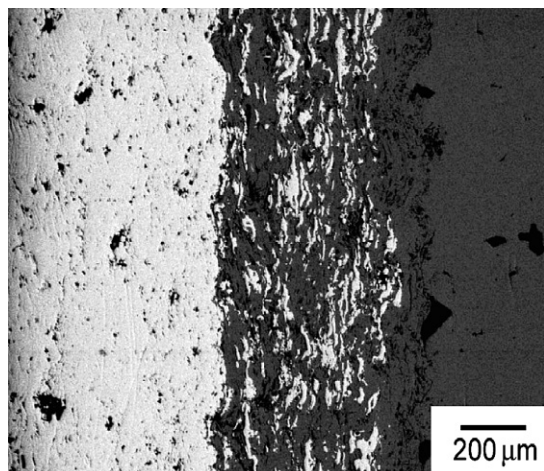


Fig. 1. SEM of cross section of W/Cu coating FGM by APS.

FGM, in which the Cu components are bright and the tungsten are gray. The W/Cu interlayer coating exhibits the typical lamellar structure, formed by overlapping W and Cu splats, with the tendency to form a layered structure. The porosity of the graded interlayer was about 5% and the porosity of the pure W layer was about 12%, which was represented by the dark areas shown in Fig. 1. The bonding strength between the substrate and the coating was 23 MPa. The thermal conductivity of this W/Cu FGM was  $57 \text{ Wm}^{-1} \text{ K}^{-1}$  at room temperature.

### 3.2. W/Cu FGM by infiltration welding method

Fig. 2(a) shows the BEI of the cross section of W/Cu graded layer fabricated by infiltration method, in which the Cu components are bright and the tungsten are gray. It was noticed that nearly continuous graded distributions of compositions were found after infiltration liquid Cu into porous graded W skeleton. This kind of microstructure should be beneficial for keeping high thermal conductivity of the material. Fig. 2(b) shows the interface between the W based heavy alloy plate and the W-rich surface of W/Cu graded layer. The compositions of the gray phase near the interface (marked as 1 and 2 in the figure) are Cu, Ni and Fe according to the EDS analysis. This demonstrates that Ni and Fe have been diffused to the interface from the W-based heavy alloy side and Cu has diffused into the W plate from the W/Cu graded layer. The thermal conductivity of this W/Cu FGM was  $155 \text{ Wm}^{-1} \text{ K}^{-1}$  at room temperature.

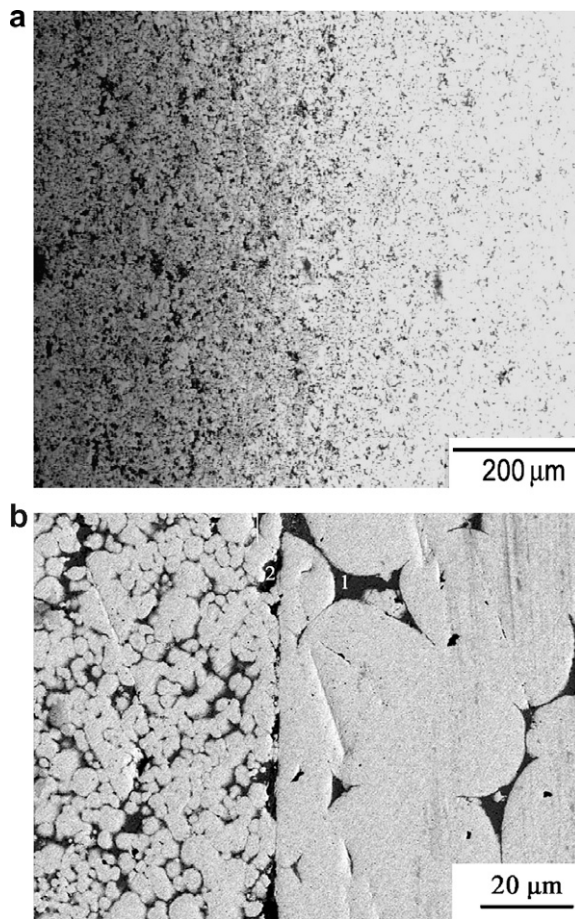


Fig. 2. Morphology of W/Cu FGM fabricated by infiltration-welding process: (a) W/Cu graded layer and (b) interface between W plate and W/Cu graded layer.

### 3.3. W/Cu FGM by RSUHP

Fig. 3(a) shows the BEI of the cross section of the 6-layered W/Cu FGM, the composition of each layer is as follows (vol.%): W100%; W80% + Cu20%; W60% + Cu40%; W40% + Cu60%; W20% + Cu80%; Cu100%, a good graded compositional transition was found. This reveals that there was no obvious composition migration during the very short sintering time. Fig. 3(b) shows the morphology of the pure W layer, it is obvious that fine W powder had been sintered and bonded well together. The relative density of pure W layer was more than 97%. The hardness of the pure W layer was 780 HV, which is much higher than pure conventional sintered W (about 350 HV). This should be due to the finer grain size of the produced W than that of the conventional sintered W. The thermal conductivity of this W/Cu

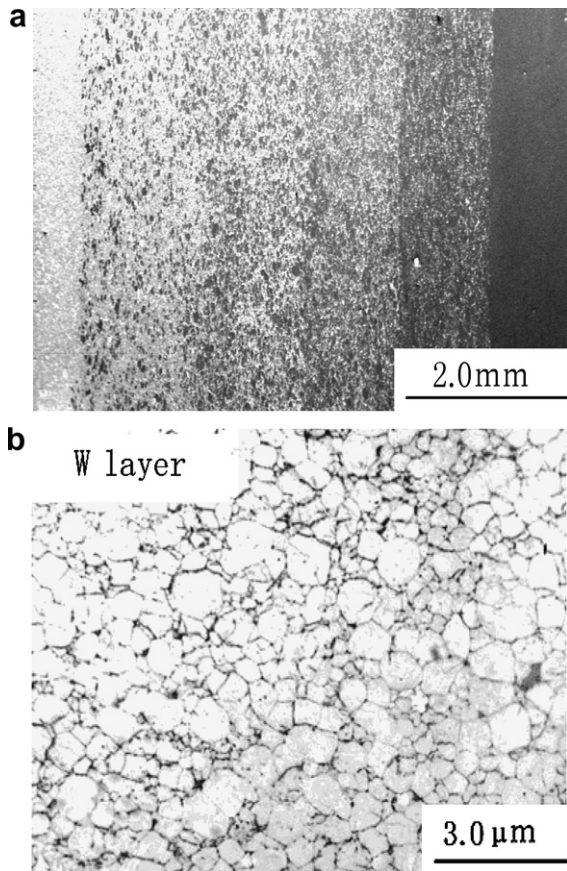


Fig. 3. SEM micrograph of cross section of six-layered W/Cu FGM and pure W layer: (a) cross section of W/Cu FGM and (b) morphology of pure W layer.

FGM was  $113 \text{ Wm}^{-1} \text{ K}^{-1}$  at room temperature. For comparison, W to Cu laminated sample was also fabricated by the same method – RSUHP.

#### 3.4. Thermal shock test

Preliminary thermal shock tests were conducted by using a muffle furnace. Samples were put into the furnace when their temperature reached to  $800 \text{ }^\circ\text{C}$ , and the holding time was 3 min. After heating, the samples were directly quenched into water, the temperature of the water throughout the cycling were between 20 and  $30 \text{ }^\circ\text{C}$ .

As to W/Cu FGM by APS, heavy oxidation occurred in the pure W coating due to its high porosity, and net-like cracks could be observed in the W part after only two quenching cycles. The W coating was broken to pieces and peeled off after the third test.

For W/Cu FGM by infiltration welding method, no obvious damage was occurred but heavy oxidation occurred in the graded layer after 30 quenching cycles.

As to W/Cu FGM by RSUHP, the integrity of the bulk material remained unaffected after 30 times of quenching, although heavy oxidation occurred in the middle layers and micro-cracks occurred in the surface of the pure W layer, as shown in Fig. 4(a). While in the case of the W to Cu laminated sample, many vertical cracks could be observed in the W part and detachment occurred at the interface between W and Cu after five quenching cycles, as shown in Fig. 4(b). The W layer was broken to pieces and peeled off after 15 times test. This demonstrated that the grading at the interface between W

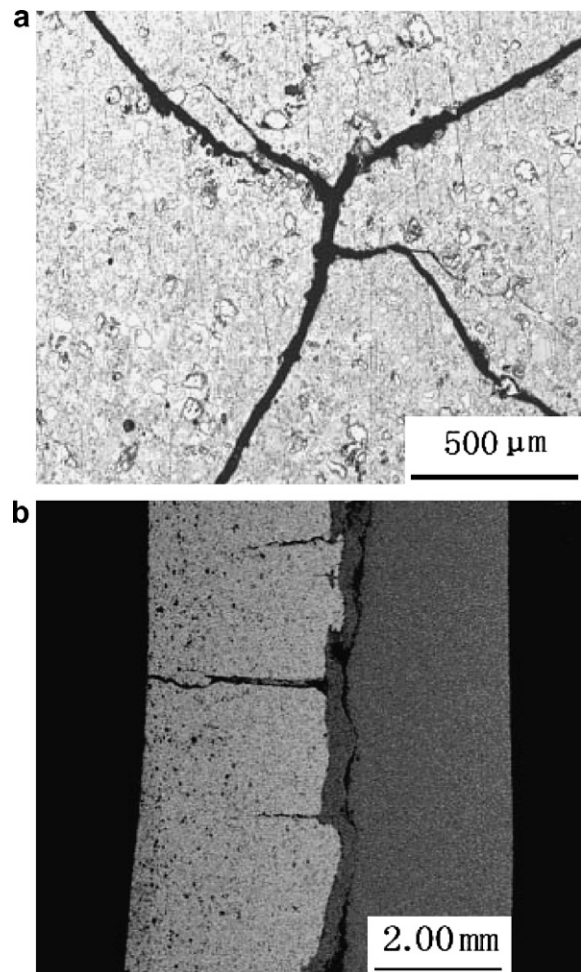


Fig. 4. Morphology of W/Cu FGM and W/Cu composite after thermal shock test: (a) surface of W/Cu FGM after 30 cycle quenching and (b) cross section of W/Cu composite after five cycle quenching.

and Cu was very effective for the reduction of thermal stress.

### 3.5. High heat flux test

An electron-beam with a 2-ms pulse width was used for high heat load tests. The energy density was  $10 \text{ MW/m}^2$ . After 1000 cycles of hot impact, micro cracks occurred in the W coating of the W/Cu FGM by APS and delamination occurred between the coating and the substrate. No obvious cracks occurred in the W/Cu FGM fabricated by the other two methods.

A Nd:YAG laser beam with a 10-ms pulse length, wave length of  $1.06 \mu\text{m}$  and frequency of 5 Hz was also used for high heat load test on W/Cu FGM samples fabricated by infiltration-welding method and RSUHP. The laser beam diameter is about 2 mm. Argon was used to protect the samples for avoiding oxidation during the test.

The bottom of the samples was immersed into flowing water. Although the laser beam was not a perfect method for high heat flux testing, it was useful for comparison of thermal resistance between samples of the same materials.

No change occurred in the surface of the tungsten with W/Cu FGM by infiltration-welding method after 2 min hot impact in air with laser energy density of  $198 \text{ MW/m}^2$ . As to W/Cu FGM by RSUHP, no crater but micro cracking occurred in the surface of the tungsten, as shown in Fig. 5(a). It should be noted that obvious crater was occurred on pure tungsten samples fabricated by RSUHP at the same testing condition. This demonstrated that W/Cu FGM has higher thermal resistance than pure tungsten. With higher energy density of  $260 \text{ MW/m}^2$  and duration of 10 s, crater morphology was found in the laser dot for all samples. The crater is enlarged when the hot impact time is increased, as shown in Fig. 5(b), which revealed larger scale evaporation during the impact process.

## 4. Conclusions and prospect

For W/Cu FGM fabricated by APS, although it has obvious beneficial features, such as in situ operation is suitable for large components and complex shapes, cost-effective, wide composition spectrum from 100 wt% Cu to 100% W can be made, but the thickness of W layer is limited, while the porosity of the W layer is  $\sim 10\%$ . The bonding strength between the coating and the substrate is low. The thermal shock resistance and performance under high heat load of this kind of W/Cu FGM is not very good. These drawbacks may restrict its use in the future's fusion reactor.

For Cu infiltration of graded W porous skeleton-welding process, the following advantages are evident: (1) Whole composition spectrum from 100% Cu to 100% W can be realized. (2) Cu network distribution is beneficial for keeping high thermal conductivity of the material. Continuously graded composite distribution without visible interface can be achieved. (3) Thickness of the W layer can be larger than 1 mm, and the performance of the W layer can be adjusted through welding different grade of W plate. The thermal shock resistance and performance under high heat load are excellent. W/Cu FGM by this method is a promising candidate for plasma facing components in the next step fusion reactor.

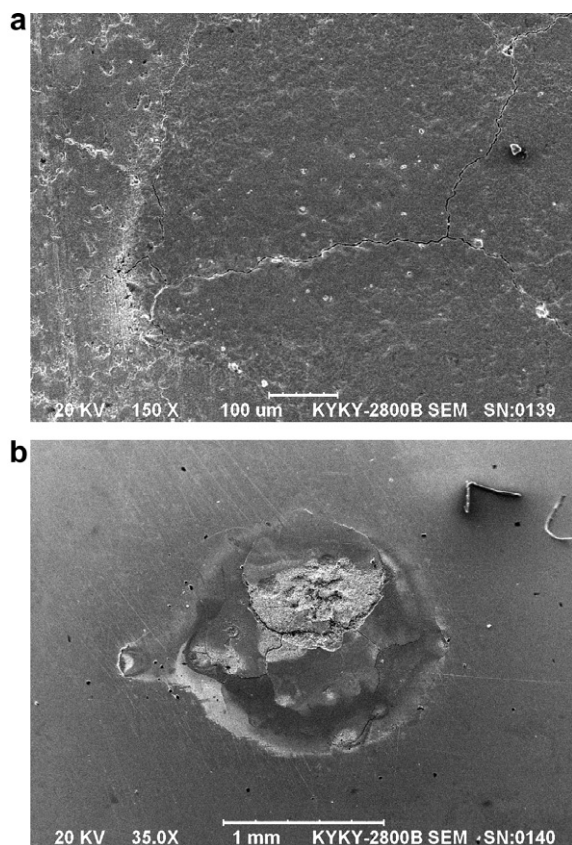


Fig. 5. SEM micrograph of tungsten surface of W/Cu FGM by RSUHP after high heat flux test: (a) energy density of  $198 \text{ MW/m}^2$ , duration of 2 min and (b) energy density of  $220 \text{ MW/m}^2$ , duration of 1 min.

For W/Cu FGM fabricated by RSUHP, its remarkable advantages are whole composition spectrum from 100% Cu to 100% W can be achieved; designed composition distributions can be kept due to short duration of graded sintering; thickness of the W layers can be larger than 1 mm and pure W layer can achieve high density even without sintering additive being added, but only small samples can be fabricated up to now. This may restrict its use from an engineering viewpoint.

### Acknowledgement

The authors would like to express their thanks for the financial support of National Natural Science Foundation of China under Grant No. 50301001.

### References

- [1] J.W. David, V.R. Barabash, A. Makhankov, et al., *J. Nucl. Mater.* 258–263 (1998) 308.
- [2] Naoaki Yoshida, *J. Nucl. Mater.* 266–269 (1999) 197.
- [3] I. Smid, M. Akiba, G. Vieider, et al., *J. Nucl. Mater.* 258–263 (1998) 160.
- [4] A. Cambe, E. Gauthier, J.M. Layet, et al., *Fus. Eng. Des.* 56&57 (2001) 331.
- [5] J. Chapa, I. Reimanis, *J. Nucl. Mater.* 303 (2002) 131.
- [6] C.C. Ge, J.T. Li, Z.J. Zhou, et al., *J. Nucl. Mater.* 283–287 (2000) 1116.
- [7] Y. Itoh, M. Takahashi, H. Takano, *Fus. Eng. Des.* 31 (1996) 279.
- [8] G. Pintsuk, S.E. Bruinings, J.-E. Doring, et al., *Fus. Eng. Des.* 66 (2003) 237.
- [9] Y.H. Ling, J.T. Li, Z.J. Zhou, C.C. Ge, *J. Univ. Sci. Technol. Beijing* 8 (2001) 198.
- [10] Z.J. Zhou, Y.S. Kwon, *J. Mater. Process. Technol.* 168 (2005) 107.